Optics Communications 325 (2014) 60–67

Contents lists available at ScienceDirect

Optics Communications

journal homepage: www.elsevier.com/locate/optcom

Duplex self-mixing interference based on ultra-narrow linewidth fiber ring laser

Zhengting Du [a], Liang Lu [a,*], Shuang Wu [a], Wenhua Zhang [a], Bo Yang [a], Rong Xiang [a], Zhigang Cao [a], Huaqiao Gui [b], Jianguo Liu [b], Benli Yu [a]

[a] Key Laboratory of Opto-Electronic Information Acquisition and Manipulation of Ministry of Education, Anhui University, Jiulong Road 111#, Hefei 230601, China

[b] Key Laboratory of Environmental Optics and Technology, Anhui Institute of Optics and Fine Mechanics, Chinese Academy of Sciences, Hefei 230031, China

ARTICLE INFO

Article history:
Received 14 October 2013
Received in revised form
20 March 2014
Accepted 23 March 2014
Available online 3 April 2014

Keywords:
Fiber laser
Self-mixing
Laser sensor

ABSTRACT

A novel duplex self-mixing interference based on ultra-narrow linewidth fiber ring laser is investigated. Dense Wavelength Division Multiplexing (DWDM) is applied to add-drop the dual-channel vibration signal into the fiber laser. Meanwhile, the output power with optical feedback is theoretically deduced which can not only be interpreted by the well known expression of self-mixing interference but the combination of self-mixing interference and mode competition. Experimental results show that different movements of each channel detected from the dual-channel fiber laser self-mixing interference system are in good agreement with theoretical analysis. Furthermore, a novel system measuring 2-dimensional vibration is introduced in this paper and its potential application to self-mixing interference measurement system for high sensitivity, remote and multi-dimensional measurement is shown.

1. Introduction

Er^{3+} doped fiber (EDF) is effective for fiber ring lasers (FRLs) as it increases gain spectrum in both C-band and L-band [1–3]. Multi-wavelength fiber ring lasers (MFRLs) based on EDF appeal researchers for their potential applications in Dense-Wavelength-Division-Multiplexing (DWDM) optical communication systems, optical fiber sensors, surveillance and optical instrument testing due to their narrow linewidth, high power, low intensity noise, nearly diffraction limited beams, reliability, intrinsic safety, electromagnetic interference immunity, capability for remote control and low transmission loss [3–5]. Actually, EDF is not only an excellent gain medium but also an excellent saturable absorber [6–7,12] to narrow the fiber laser linewidth due to a super narrow band filter constructed by the un-pumped Erbium-doped fiber with high reflectivity fiber Bragg grating. The narrow linewidth is critical to coherence length limitation, high performance of self-mixing measurement system based on MFRLs that has rarely been reported so far.

Recently self-mixing interference (SMI) [8–14] has drawn much attention of researchers in optical sensor application due to its smart, easy alignment, high accuracy and reliability compared to the traditional heterodyne interference technologies, such as Michelson interference technology and Mach–Zehnder interference technology. SMI occurs when the light scattered by the object diffusing surface reenters the laser cavity. The feedback light modulates the gain and the frequency of the laser, so the amplitude and frequency of the object can be obtained through the demodulated processing circuit where one fringe shifting corresponds to a displacement of $\lambda/2$. Obviously novel multi-channel measurement could be realized in MFRL with ultra-narrow linewidth essential to remote, distributed, multi-parameter sensor by the SMI technique when a DWDM device is employed to split the lasing beam into multi-channel single wavelength light.

In this paper, we propose a novel dual-channel SMI vibrameter to obtain stable and high SNR self-mixing interference signals on the base of ultra-narrow linewidth dual wavelength ring erbium-doped fiber laser potentially applied to remote, distributed, multi-parameter sensors. In Section 2, we build a traditional three-mirror model to explain the SMI phenomena and propose the scheme of dual-channel vibrameter. In Section 3, the highly sensitive and stable results of vibration based on SMI are experimentally observed and theoretically analyzed by the combination of self-mixing interference and the model of Giles [15].

2. Principle

In this part a traditional three-mirror model [9,11] is introduced to the self-mixing vibrameter firstly. Both the gain and the

* Corresponding author.
E-mail address: Lianglu@ahu.edu.cn (L. Lu).

http://dx.doi.org/10.1016/j.optcom.2014.03.070
0030-4018/

frequency of the laser are affected by the feedback light; hence, the modulated output power of the laser is related to external object vibration characteristics. Assuming one wavelength light would not interfere with the other lasing light in the dual-channel vibrameter investigated in the paper, the dual-channel vibration separately obtained as one wavelength self-mixing interference is analyzed. Fig. 1 shows a molding sketch of three-mirror laser lasing at single wavelength with an external cavity. r_1, r_2, and r_3 are reflection coefficients of the front (M_1), rear (M_2), and external (M_3) mirror respectively. L_{in} represents the length of the lasing cavity, while L_e is the distance from the rear mirror to the external mirror. In the process of solving the electric field equation and the phase condition based on the stationary stable laser oscillation, the equivalent cavity model is introduced in the traditional three-mirror model to obtain the results of self-mixing interference in which the rear (M_2) and external (M_3) mirrors are replaced by an equivalent mirror with a coupling coefficient of ζ [9]. In case of one-way reflection, $|r_3| \ll |r_2|$ and the external target is driven by a sinusoidal signal with the angular frequency of w_0 and amplitude of A; we can now derive expressions for the change of threshold gain and laser frequency with feedback.

$$\Delta\nu = \frac{C\ \sin(2\pi\nu\tau_e + \arctan\partial)}{2\pi\tau_{in}} \tag{1}$$

$$\Delta g = -\frac{\xi}{L_{in}}\ \cos(2\pi\nu\tau_e) \tag{2}$$

Eqs. (1) and (2) respectively, describe the change of laser frequency (ν) and threshold gain (g) resulting from steady-state amplitude and phase equations of lasing condition based on the self-mixing interference. Δg and $\Delta\nu$ represent the change of threshold gain and frequency in the laser with feedback. τ_{in} and τ_e are the time of a round-trip through inner cavity and external cavity, respectively. ∂ and C represent the line-width enhancement factor and the external feedback strength, respectively. Based on Eqs. (1) and (2) the laser intensity can be expressed as [11]

$$I = I_0(1 - \kappa\Delta g) \tag{3}$$

Here, κ is related to the operation parameters. From Eqs. (1)–(3), we can obtain the output power of the laser with feedback and Eq. (3) can be expressed as

$$I = I_0\left(1 + m\ \cos\left(4\pi\nu\left(\frac{L_e + A\ \cos(2\pi w_0 t))}{c}\right)\right)\right) \tag{4}$$

I_0 represents the output power without feedback. One fringe shifting corresponds to a displacement of $\lambda/2$; the frequency can be obtained by the period of SMI signal. Apparently we can easily calculate and obtain the vibration information through the self-mixing interference fringes in Eq. (4). Provided one wavelength light would not interfere with the other lasing light, the dual-channel vibration signal can be independently achieved as shown in the following equation by the three-mirror model:

$$I_i = I_{i0}\left(1 + m_i\ \cos\left(\frac{4\pi\nu(L_{ie} + A_i\ \cos(2\pi w_{i0} t))}{c}\right)\right) \tag{5}$$

where the subscript i denotes the related parameter of the i sensing channel. When DWDM is adopted to separate the multi-wavelength lasing light into multiple sensing channels, the multiple sensors can be realized with non-interference based on the self-mixing interference inside an MFRL.

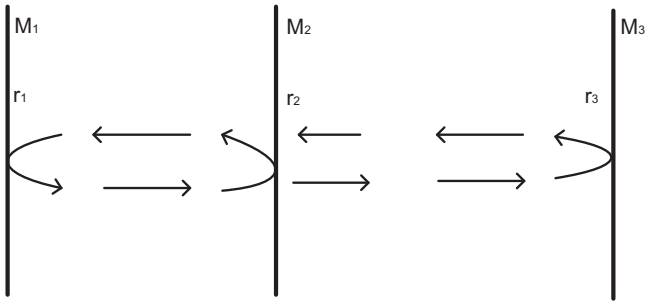

Fig. 1. Sketch of three-mirror model of self-mixing interference.

3. Experimental results and discussion

3.1. The experimental setup of duplex SMI vibrameter based on dual-wavelength ultra-narrow linewidth fiber laser

In this section, the outstanding coherency source is applied to the dual-channel self-mixing interference to study the external target vibration. In the experimental setup schematically shown in Fig. 2, a duplex SMI vibrameter consists of a dual independent wavelength fiber ring laser (DFRL), a dual-channel light emission and collection system, two speakers with diffusing surfaces driven by two different signals of function generators and parallel processing circuits to process the SMI signals. To realize the DFRL, a DWDM is employed to divide dual-wavelength lasing light into two independent wavelength light sources. The dual-channel light emission and collection

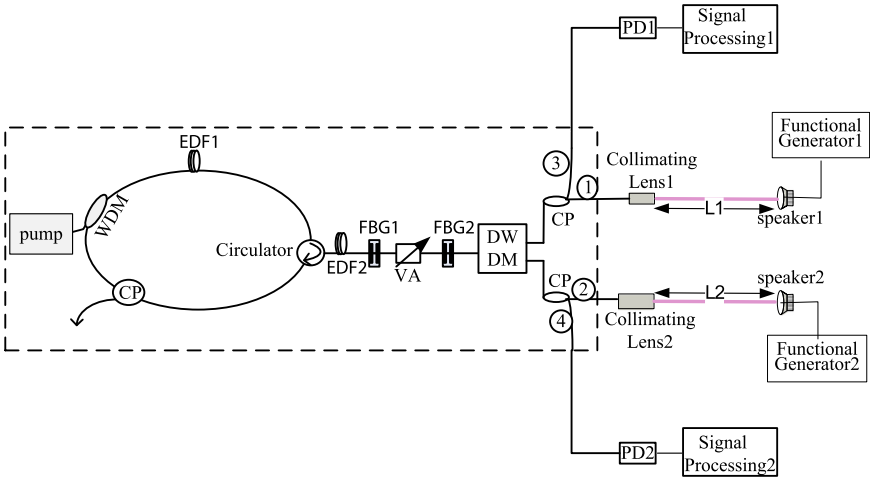

Fig. 2. Experiment setup of self-mixing vibrameter based on DFRL.

system is two separate collimators to lase the collimation light and receive the backscattered light of the vibration objects.

The schematic of dual-wavelength ultra-narrow linewidth fiber ring laser to optimize the SMI measurement system in Fig. 2 is labeled by a dashed box, where two segments of Fiber Bragg Grating (FBG) are employed to filter the lasing wavelength, two sections of EDF are used as both a gain medium and a narrowband reflection filter. The mechanism of linewidth narrowing is to establish a transient auto-tracking filter by standing-wave saturation effects in the un-pumped EDF_2. The induced EDF_2 could serve as a mode selection and suppress frequency hop. A WDM coupler is applied to launch the pump power into the EDF_1. The stimulated gain medium (EDF_1) amplifies the signals of λ_1 and λ_2 chosen by the mode selecting apparatus of FBG_1 and FBG_2 with Bragg wavelengths of 1549.7 nm and 1539.6 nm. The bandwidth and grating diffraction efficiency reflectances of FBG1 and FBG2 are 0.285 nm and 0.213 nm, 87% and 90% respectively. The circulator ensures unidirectionality of the light and prevents unwanted feedback within the ring. A variable optical attenuator (VA) is a device to balance the mode competition between λ_1 and λ_2. The saturable absorber of un-pumped EDF_2 is inserted between the circulator and the FBGs, which is the key component guaranteeing a steady, narrow linewidth and outstanding coherency source. DWDM joins multiplex signals together and demultiplexes them apart. So we can manufacture a DFRL that functions as an optical add-drop multiplexer to measure the dual-channel vibration. The DWDM demultiplexes the dual-wavelength of MFRL into two independent lasing lights of λ_1 and λ_2. The 1st and 3rd ports connect to the collimator lens1 and the signal processing circuit1 with wavelength of λ_1 in channel1. The 2nd and 4th ports of channel2 are related to the wavelength of λ_2. The feedback light scattered by the target is coupled into the DFRL by the dual-channel light emission and collection system of collimating lens1 and collimating lens2. The external diffusing surfaces fixed on two speakers are driven by two different signals of function generators with different lengths away from collimating lenses. CPs are couplers to obtain the lasing light output.

3.2. The stable output of the dual independent wavelength fiber ring laser

To steady the narrow linewidth and outstanding coherency source of dual independent wavelength lasing, the VA, EDF_2, and DWDM are introduced. Here the VA reduces the power level of λ_2 to balance the mode competition and lets the gain and loss of λ_1 and λ_2 satisfy the Giles model [15], referred to

$$l_2 + \mathrm{VA} = l_1 \frac{\alpha_2 + g_2^*}{\alpha_1 + g_1^*} + (10lge)\frac{\alpha_2 + g_2^*}{\alpha_1 + g_1^*}\alpha_1 L - (10lge)\alpha_2 L \quad (6)$$

Subscripts 1 and 2 denote the signal light of λ_1 and λ_2, respectively, α and g^* are absorption and gain spectra of EDF, respectively. In the experiment, L is the length of the EDF_1, which is equal to 4.2 m. l_1 and l_2 refer to the total attenuation factor including splicing and insertion loss of WDM, circulator and other optical components. In Eq. (6), we can figure out the value of VA to balance the dual wavelengths mode competition. According to the loss and boundary condition of each wavelength signal light, the dual wavelengths synchronous oscillate and generate sharp peaks when the condition is satisfied; otherwise either one signal light would be chosen while the other one would be suppressed.

Fig. 3 shows the typical spectrograms of DFRL obtained at spectrograph (Yokogawa AQ6370C Optical Spectrum Analyzer) where the SNR up to 70 dB is determined by the amplified spontaneous emission (ASE). Fig. 3a is the spectrum of dual wavelengths synchronous oscillate with an output power difference of 0.19 dBm and the wavelength spacing of 10.048 nm, which

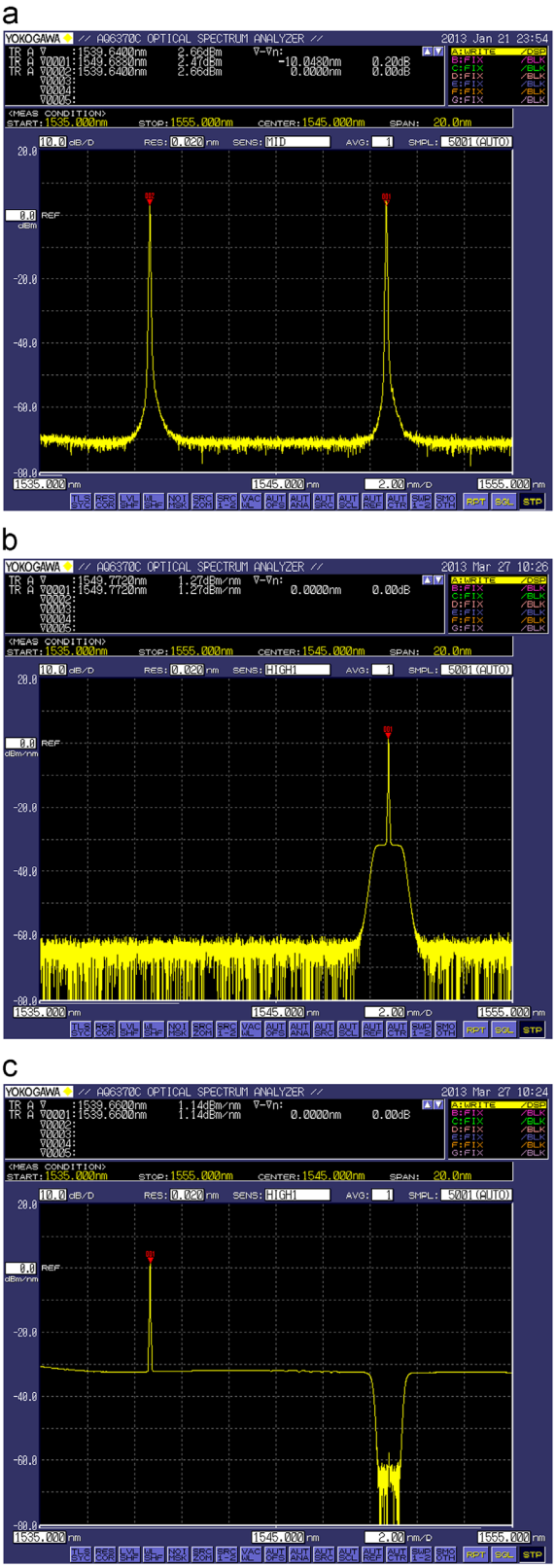

Fig. 3. The typical emission spectrum obtained at spectrograph. (a) The typical emission spectrum of dual wavelengths, (b) the emission spectrum of the fiber laser at 1549.77 nm, and (c) the emission spectrum of the fiber laser at 1539.66 nm.

depends on the wavelength of FBGs available. The dual wavelength would be demultiplexed into two independent lasing lights by the DWDM as shown in Fig. 3b and c. Here the DWDM could also multiplex the dual channel scattered light to the laser cavity so that the phenomenon of SMI would occur.

The spectral lineshapes of the laser shown in Fig. 4 are investigated by a homodyne technique using a fiber Mach–Zehnder interferometer with a 20 km delay-line in one arm. The beat signals from the interferometer, which are detected by a photoreceiver and a spectrum analyzer (Tektronix RSA-3408B Real-Time Spectrum Analyzer). The fall at low frequencies is caused by the low-frequency filter in the photoreceiver. Curve fittings are used to figure out the measured values shown in Fig. 4 by the red dotted lines. As shown in Fig. 4 the drastically narrow linewidth of the novel system that with unpumped EDF_2 is 428.25 Hz and 878.4 Hz at 1539.66 nm and 1549.77 nm respectively. A linewidth of 1 kHz corresponds to a coherence length of 300 km, which is larger than the delay-line length. Therefore, the linewidth of the laser output is less than the measured values. It is indicated that the employment of EDF_2 would guarantee the narrow linewidth operation, which is significant for potential remote sensing, and stable and high SNR signal in the novel SMI sensing system.

3.3. *The experimental results of duplex self-mixing interference in the dual independent wavelength fiber ring laser*

In our SMI experimental setup, two fast InGaAs photodiodes are connected to port 3 related to channel1 and port 4 associated with channel2 in DFRL to observe the dual channel experimental signals of SMI. As a “fringe” shifting corresponds to a 2π phase shift caused by the vibration of the external object, a typical dual-channel SMI signal is obtained when the targets are driven by sinusoidal signals as shown in Fig. 5. The dual-channel external speakers are driven by function generators with different signals. Channel1 is illuminated by 1549.77 nm and the voltage added on speaker1 is a sinusoidal signal with the frequency of 230 Hz and driving voltage 28 mVpp as shown in trace3 in Fig. 5. At the same time the lasing light on channel2 is 1539.66 nm and the sinusoidal signal that launches at the speaker, which is shown as trace4, is 280 Hz 85 mVpp. Trace1 and trace2 are the SMI signals of channel1 and channel2, respectively, as observed on an oscilloscope (Tektronix DPO 2024 Digital Phosphor Oscilloscope).

Fig. 5a shows the novel experimental result of output which is recorded by an oscilloscope with different target movements. Self-mixing interference signal of 1549.77 nm is modulated by the backscattered light of speaker1 and there are seven fringes in the driven period, and a self-mixing interference signal of 1539.66 nm is modulated by a feedback light of speaker2 and there are 5 fringes in the driven period. The phenomenon of mode competition of the two channels is also observed. It is clear that different movements can be detected from the self-mixing interference in fiber ring laser with a parallel dual-channel, and hence the remote, distributed multi-parameter sensor can be potentially obtained in the novel SMI system with ultra-narrow linewidth fiber ring laser. In our dual-channel vibrameter system, the signals are processed by trans-impedance amplifier, filter and further amplifier. To enhance the signal-to-noise ratio, electronic band-pass filters are used. Then a following amplifier makes the signal large enough to be observed by the oscilloscope for obtaining the vibrational property of the loud speakers.

Research is still being carried out to fully understand the phenomenon in the experiments. Assumed in the theory part, the dual-channel vibration would be separately obtained as one wavelength self-mixing interference does not interfere with the other wavelength scattered light. Therefore, each channel's self-mixing interference signal would be the same as the single channel's self-mixing interference signal as shown in Fig. 5b and c. Fig. 5b shows the self-mixing signal with one channel switched on (channel1: 230 Hz, 28 mV; channel2: switched off) and Fig. 5c shows the signal with the other channel switched on (channel1: switched off; channel2: 280 Hz, 85 mV). However, the self-mixing interference signal observed in the dual-channel vibration measurement system as shown in Fig. 5a deviates from the conclusion of assumption though the dual-channel movements can be acquired from the self-mixing system in the fiber ring laser.

To deeply understand the theory model of dual-channel self-mixing interference in a DFRL, we compare Fig. 5a and b; Fig. 5c and find that the self-mixing signal can not only be analyzed by the three-mirror model, but also the mode competition should be considered.

To get a full appreciation of self-mixing interference of λ_1 and λ_2, which is different from the assumption in the theory part, the

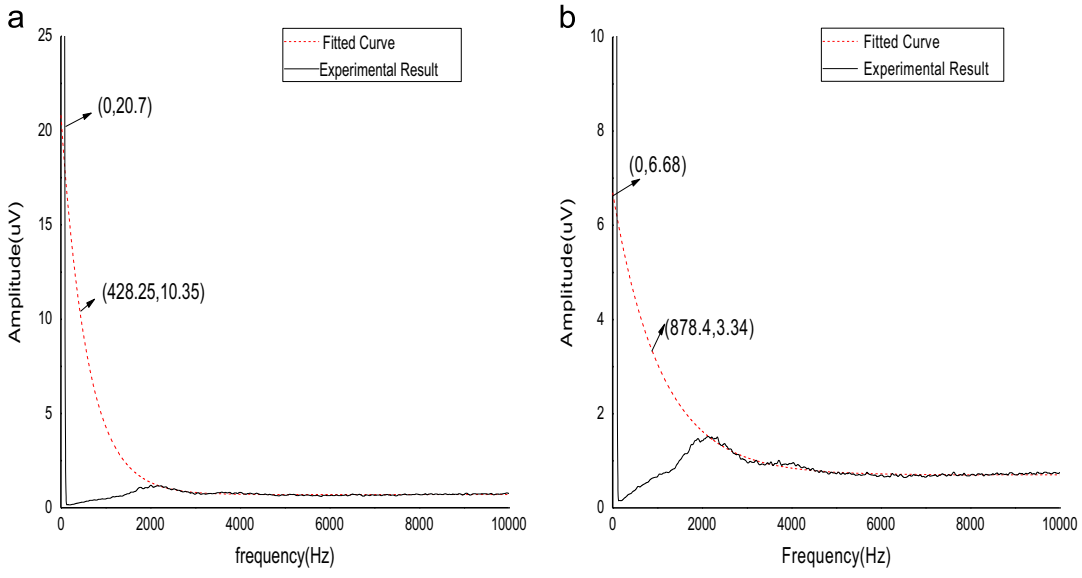

Fig. 4. Lineshape of the homodyne signal measured with 20-km delay and theoretical Lorentzian approximation (dotted line). (a) The linewidth is 428.25 Hz at 1539.66 nm and (b) the linewidth is 878.4 Hz at 1549.77 nm.

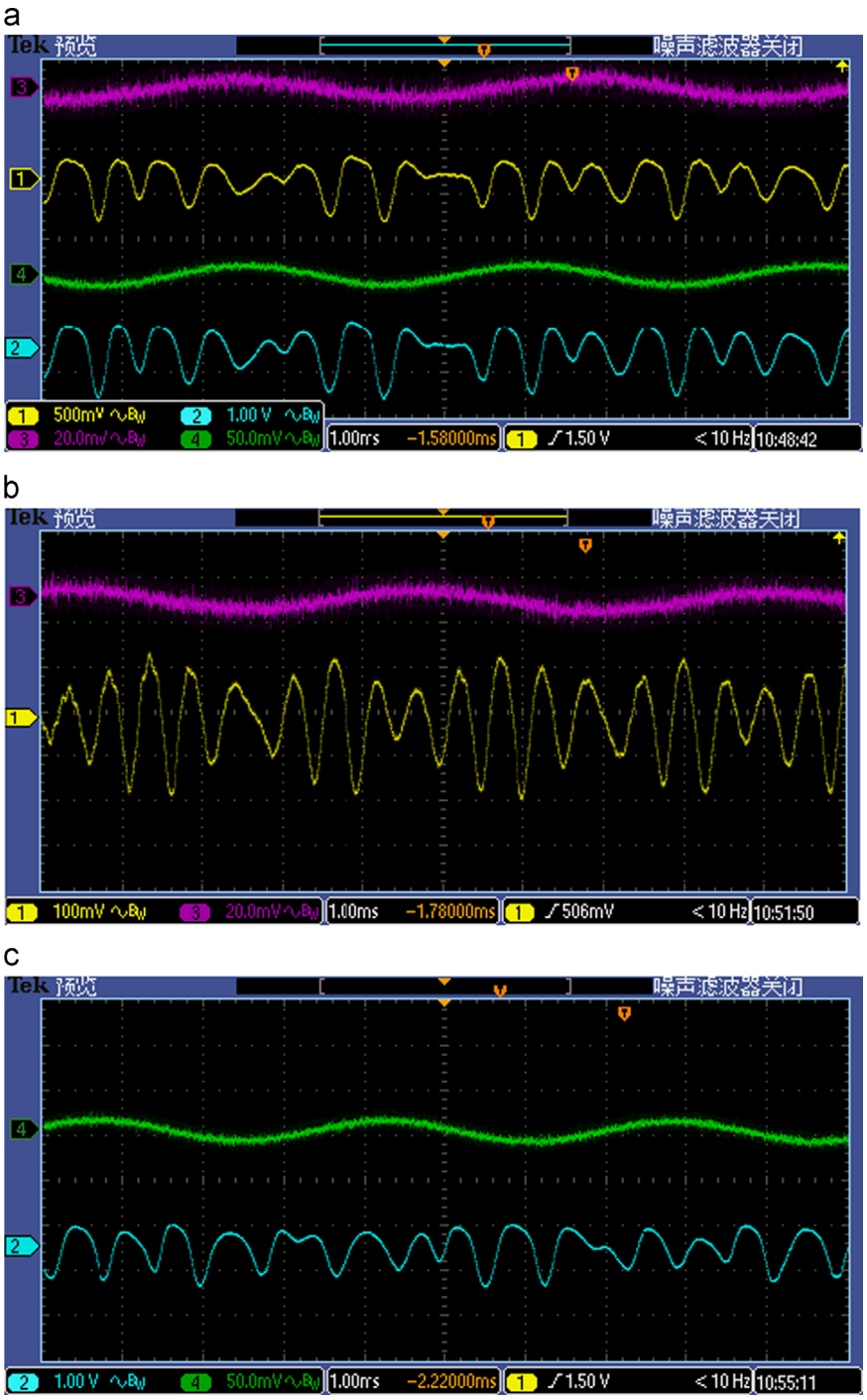

Fig. 5. Self-mixing signals of dual-channel vibration measurement system. (a) Self-mixing signal with both channel switched on (channel1: 230 Hz, 28 mV; channel2: 280 Hz, 85 mV), (b) self-mixing signal with one channel switched on (channel1: 230 Hz, 28 mV; channel2: switched off), and (c) self-mixing signal with one channel switched on (channel1: switched off; channel2: 280 Hz, 85 mV).

Giles model [15] is introduced to analyze the mode competition and revise the theory part.

$$\frac{\Delta g_1}{\Delta g_2}=\frac{\alpha_1+g_1^*}{\alpha_1+g_1^*} \tag{7}$$

In this case the change of λ_1 overall gain modulated by the reentering of light of channel1 would synchronously affect the gain variation of λ_2 and vice versa due to the homogeneous broadening of EDF at room temperature. Here the modulated output power of λ_1 and λ_2 would be impacted by the reentering light of channel1 and channel2. Replace Eqs. (1) and (2) in dual channel measurement with the following equations:

$$\Delta v=\frac{C\ \sin(2\pi v\tau_e+\arctan\partial)+\partial m_i\xi_i\ \cos(2\pi v_i\tau_{ei})}{2\pi\tau_{in}} \tag{8}$$

$$\Delta g=-\frac{\xi}{L_{in}}\cos(2\pi v\tau_e)-m_i\frac{\xi_i}{L_{ini}}\cos(2\pi v_i\tau_{ei}) \tag{9}$$

where the subscript i is the influence of the other channel and the parameters without subscript i represent the change caused by the feedback light of its own measured object, m_i is the gain ratio of the i channel to its initial.

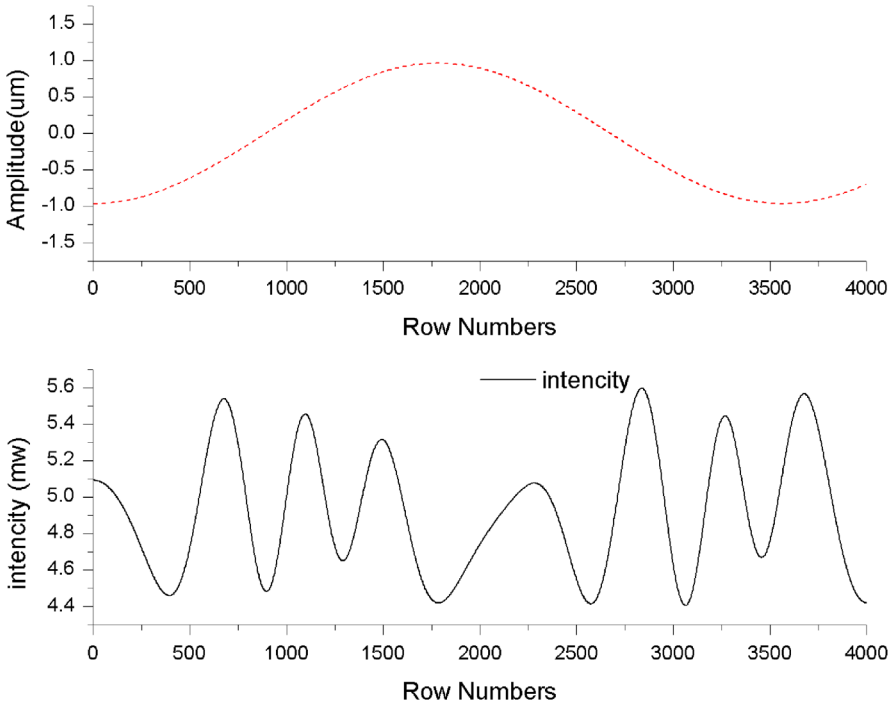

Fig. 6. Simulation result of output variation in dual-channel with the different frequency and amplitude of target movements (channel1: the black line, 230 Hz 1.356 μm, channel2: the red dashed line, 280 Hz 0.962 μm).

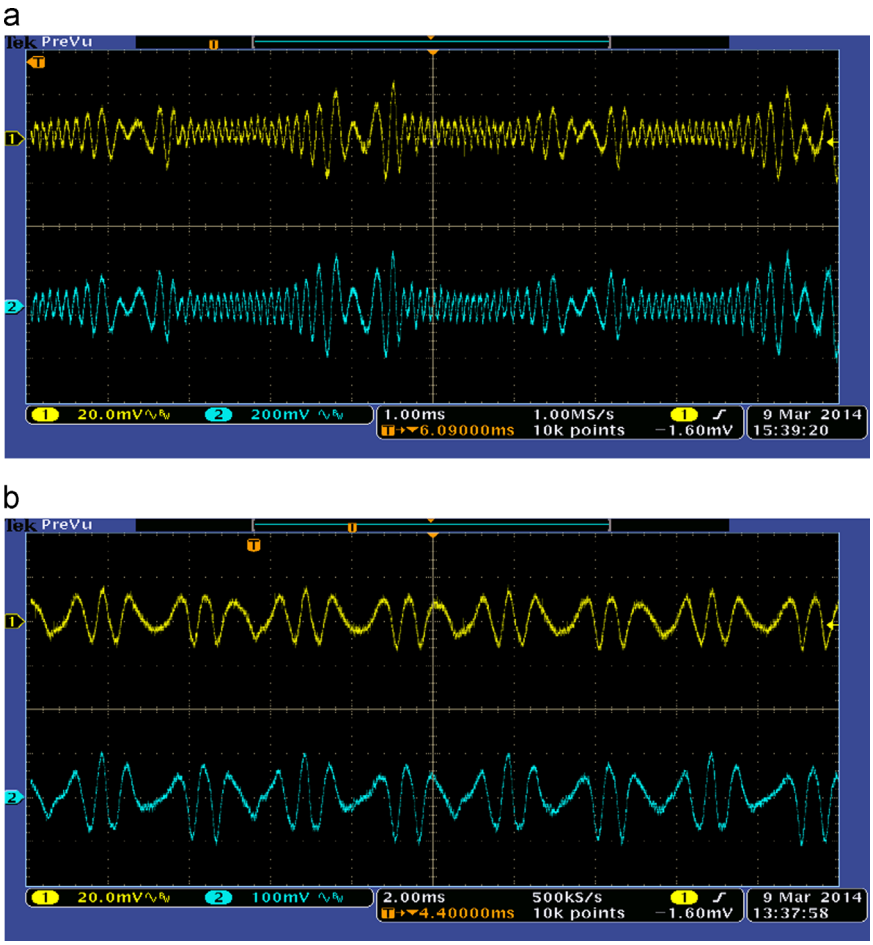

Fig. 7. Duplex self-mixing interference signals with one channel switched on. (a) Duplex self-mixing interference signals with one channel switched on (channel1: 190 Hz 95 mVpp; channel2: switched off) and (b) duplex self-mixing interference signals with one channel switched on (channel1: switched off; channel2: 200 Hz 55 mVpp).

Given the Giles model of mode competition in the dual channel vibrameter system, the output power can be obtained from the numerical solution to Eq. (3).

To confirm the interpretation of the physical meaning in the dual channel vibrameter system observed by the combination of three-mirror model and mode competition, the output power can be derived from Eq. (3) based on Eqs. (8) and (9). The output power calculated is in good agreement with the experimental results in the whole time-domain as shown in Fig. 6. In Fig. 6 the upper traces are the driven signals with different amplitudes and frequencies launched to achieve the periodic movement of each external reflector. The lower trace is the output power of the dual-channel self-mixing interference in a dual independent wavelength fiber ring laser (DFRL) where the seven fringes in channel1 driven period and five fringes in channel2 driven period. Through the mode competition of self-mixing interference in the DFRL, the vibration information of each channel can be achieved by the output power of the DFRL using the SMI technique.

The fiber laser adopted in the experimental setup would be either one signal light lasing while the other one would be oppressed when the value of VA does not fulfill Eq. (6). Therefore we experimentally operate the value of VA to unbalance the dual wavelengths synchronous oscillate but to generate a sharp peak of either one wavelength signal light. When the condition is satisfied, the only running sensor channel would be channel1 or channel2. So the novel sensor setup applied in the paper could be functioned as the dual-channel switchable vibrameter which has been experimentally realized and the stability, high SNR of the self-mixing signals are obtained with external cavity of both 50 m and 2 km, which agree with Ref. [12]. Although the simple sum in Eqs. (8) and (9) influences the output powers derived from mode competition, the vibration information of each channel can still be achieved during its own driven period as shown in Figs. 5 and 6. Additionally, the novel SMI sensor system based on narrow linewidth laser in this paper has a number of potential applications for high performance in remote, distributed multi-parameter self-mixing measurement and differential measurement. Furthermore to achieve the single pure SMI signal assumed as the theory part, the signals need to be processed by subsequent signal processing circuits which need intensive study.

To illustrate the output power of the duplex self-mixing interference based on ultra-narrow linewidth fiber ring laser is theoretically deduced by a combination of self-mixing interference and mode competition; we measure dual-wavelength self-mixing interference signals shown in Fig. 7 on condition that the value of VA is set to satisfy Eq. (6) and the mode competition between the dual wavelength lasing light is intense. Trace1 and trace2 in Fig. 7 are the SMI signals of 1549.77 nm and 1539.66 nm, respectively, as observed on oscilloscope.

As shown in Fig. 7, the duplex self-mixing interference signals with one channel switched on are obtained resulting from a phase modulation of one sensing channel by the signal generator launched on the related speaker. Fig. 7a shows the duplex self-mixing interference signal with one channel switched on (channel1:190 Hz 95 mVpp; channel2: switched off). Self-mixing interference signal of 1549.77 nm is modulated by the backscattered light of speaker1 and there are 48 fringes in the driven period as shown in Fig. 7a by trace1 while the mode competition affects the gain and frequency of lasing light at 1539.66 nm; thus the self-mixing interference of 1549.77 nm affects the output power of 1539.66 nm related to Eqs. (8) and (9). The output power of 1539.66 nm is shown in Fig. 7a by trace2 in which there are also 48 fringes in the driven period. To describe the self-mixing interference of 1539.66 nm that would impact the output power of 1549.77 nm, the duplex self-mixing interference signals with one channel switched on (channel1: switched off; channel2: 200 Hz 55 mVpp) are shown in Fig. 7b. The backscattered light of 1539.66 nm is modulated by speaker2 with 200 Hz 55 mVpp voltage driven on and the self-mixing interference of 1539.66 nm comes up as shown in Fig. 7b trace2. The scattered light of 1539.66 nm modulated the gain and frequency of 1539.66 nm as Eqs. (1) and (2) show; at the same time the mode competition of the fiber ring laser changes the gain and frequency of 1549.77 nm. Thus the fluctuated output power of the dual wavelength is simultaneously obtained as shown in Fig. 7b, in which the 6 fringes in the driven period illustrate the valid interpretation of the duplex self-mixing interference in Eqs. (8) and (9). Thus the duplex self-mixing interference with one channel switched on can achieve the dual wavelength simultaneously sensor. In the common sense, the dual wavelength would not interfere with each other, and thus the duplex self-mixing interference in fiber ring laser can be used in

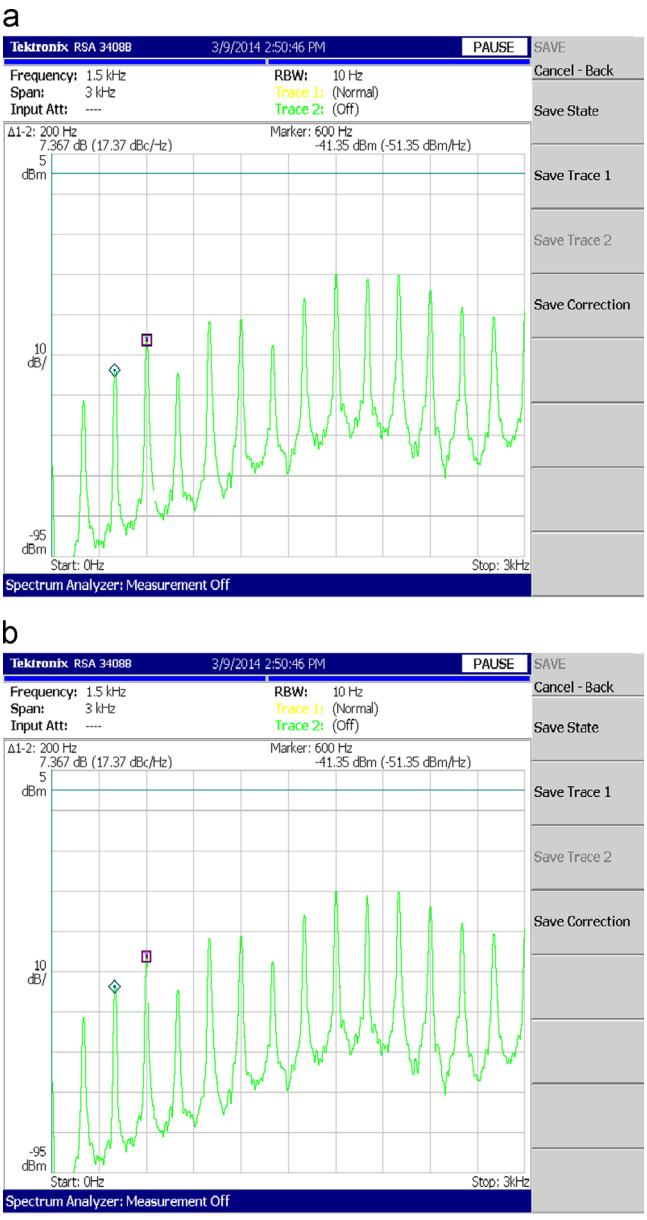

Fig. 8. Duplex self-mixing interference spectrum signals. (a) Duplex self-mixing interference spectrum signal of 1549.77 nm with one channel switched on (channel1: 200 Hz 65 mVpp; channel2: switched off) and (b) duplex self-mixing interference spectrum signal of 1539.66 nm with one channel switched on (channel1: 200 Hz 65 mVpp; channel2: switched off).

Table 1

Driven frequencies (Hz)	Measured values			
	1539.66 nm		1549.77 nm	
	Mean value (Hz)	Standard deviation	Mean value (Hz)	Standard deviation
(a) *The measured frequencies changed with the driven signals with channel1 switched on*				
120	119.368	0.865402	119.424	0.78872
160	159.6852	0.823915	159.6852	0.823915
200	200	0	200	0
240	240.964	1.835873	239.992	0.017889
280	279.666	0.323697	280.26	0.35602
320	319.368	0.865402	319.368	0.865402
360	359.768	0.317679	360.134	0.36025
(b) *The measured frequencies changed with the driven signals with channel2 switched on*				
120	119.654	0.777676	119.624	0.624564
160	159.8852	0.382407	159.8852	0.382407
200	200	0	200	0
240	240.364	1.084634	240	0.028284
280	279.866	0.53083	280.13	0.543829
320	319.768	0.77519	319.338	0.84025
360	359.968	0.356258	359.924	0.397656

remote sensor, medical and security applications such as real-time voice reproduction for spy systems.

To confirm the high performance of duplex self-mixing interference, the corresponding electric signals detected by the photodiode were delivered to a radio-frequency spectrum analyzer (Tektronix RSA-3408B Real-Time Spectrum Analyzer). Fig. 8 shows the power spectrum of the dual wavelength with one channel switched on (channel1: 200 Hz 65 mVpp; channel2: switched off) and the sweep central frequency and the sweep span of the real-time spectrum analyzer are set at 1.5 kHz and 3 kHz, respectively. A few of its vibration frequencies (200 Hz) and some FM sidebands such as 400 Hz, 600 Hz and others stand out in the duplex self-mixing interference power spectrum as shown in both Fig. 8a and b. The phenomenon occurs because of the amplitude-frequency response by the self-mixing interference. In terms of the amplitude of the vibration larger than 1/8 wavelength, the SMI signal is not a monofrequency signal but has multiple frequencies. For the sake of the ultra-narrow linewidth of the fiber ring laser, we achieved a signal-to-noise ratio (SNR) of about 40 dB based on the optimized system, which corresponds to the recent study [12].

To study the repeatability, stability and accuracy of the dual channel vibrameter, the standard deviation for five consecutive scans is calculated for each measurement frequency. The measured frequencies are the fundamental frequencies of the power spectrum due to the vibration frequencies that are manifested as fundamental frequencies. We list the measured frequencies in Table 1, which changed with the driven signals at the range of 120–360 Hz with 65 mVpp amplitude. In Table 1, the dual channel simultaneous measurement shows high accuracy in which the measured frequencies are in the vicinity of the driven frequencies, resulting from the 10 Hz Resolution Band Width (RBW) in the spectrum analyzer. Thus the duplex self-mixing interference is a valid vibrameter technique which can not only be applied to the dual channel measurement and one channel measurement such as voice measurement but also be potentially used in remote sensor.

4. Conclusion

We demonstrate a theory analysis and experimental results of duplex self-mixing interference based on a dual independent wavelength fiber ring laser (DFRL) with ultra-narrow linewidth which has never been studied. To investigate the DFRL, the DWDM is used to split the dual wavelength into dual independent wavelength lasing source and the EDF_2 is employed to obtain an ultra-narrow linewidth, which is important to the remote sensor. Different movements of the external target in each channel can be detected from the self-mixing interference system based on DFRL and the experimental results coincide with the theoretical analysis. In this paper, the theoretical model which is first proposed gives a proper interpretation on dual channel self-mixing interference in a dual wavelength fiber laser due to the mode competition in the gain medium. We have experimentally deduced the novel system with a steady, narrow linewidth and outstanding coherency source, which could provide a stability signal in the SMI measurement system. The self-mixing model of DFRL with narrow linewidth employed in this paper has potential application in remote, distributed multi-parameter self-mixing measurement and differential measurement.

Acknowledgments

This work was supported by the National Natural Science Foundation of China (Grant nos. 61307098 and 61275165), the Educational Commission of Anhui Province of China (Grant no. KJ2013A021) and the foundation of Key Laboratory of Environmental Optics and Technology of Chinese Academy of Sciences (Grant no. 2005DP173065-2013-2).

References

[1] C. Barnard, P. Myslinski, J. Chrostowski, M. Kavehrad, IEEE J. Quantum Electron. 30 (1994) 1817.
[2] G. Ning, J. Zhou, S. Aditya, P. Shum, V. Wong, D. Lim, IEEE Photon. Technol. Lett. 20 (2008) 1606.
[3] Z. Meng, G. Stewart, G. Whitenett, J. Lightwave Technol. 24 (2006) 2179.
[4] Q. Mao, J.W. Lit, IEEE Photon. Technol. Lett. 14 (2002) 1252.
[5] J. Nilsson, Y. Lee, S. Kim, IEEE Photon. Technol. Lett. 8 (1996) 1630.
[6] S.J. Frisken, Opt. Lett. 17 (1992) 1776.
[7] M. Horowitz, R. Daisy, B. Fischer, J. Zyskind, Electron. Lett. 30 (1994) 648.
[8] Z. Du, L. Lu, W. Zhang, B. Yang, H. Gui, B. Yu, Appl. Phys. B 113 (2013) 153.
[9] W.M. Wang, W.J. Boyle, K.T.V. Grattan, A.W. Palmer, Appl. Opt. 32 (1993) 1551.
[10] L. Lu, L. Zhai, K. zhang, Z. Du, B. Yu, Opt. Commun. 284 (2011) 5781.
[11] R.C. Addy, A.W. Palmer, K.T.V. Grattan, J. Lightwave Technol. 14 (1996) 2672.
[12] L. Lu, J. Yang, L. Zhai, R. Wang, Z. Cao, B. Yu, Opt. Express 20 (2012) 10.
[13] Y.L. Lim, R. Kliese, K. Bertling, K. Tanimizu, P.A. Jacobs, A.D. Rakic, Opt. Express 18 (2010) 11720.
[14] X. Dai, M. Wang, C. Zhou, IEEE Photon. Technol. Lett. 4 (2010).
[15] C.R. Giles, E. Desurvire, IEEE J. Lightwave Technol. 9 (1991) 271.